

Dynamics of Neutrophil Aggregation in Couette Flow Revealed by Videomicroscopy: Effect of Shear Rate on Two-Body Collision Efficiency and Doublet Lifetime

Harry L. Goldsmith,* T. Alexander Quinn,* Gillian Drury,* Constantina Spanos,* Fiona A. McIntosh,* and Scott I. Simon†

*McGill University Medical Clinic, Montreal General Hospital Research Institute, Montreal, Quebec H3G 1A4, Canada, and †Department of Biomedical Engineering, University of California, Davis, California 95616-5294 USA

ABSTRACT During inflammation, neutrophil capture by vascular endothelial cells is dependent on L-selectin and β_2 -integrin adhesion receptors. One of us (S.I.S.) previously demonstrated that homotypic neutrophil aggregation is analogous to this process in that it is also mediated by these receptors, thus providing a model for studying the dynamics of neutrophil adhesion. In the present work, we set out to confirm the hypothesis that cell–cell adhesion via selectins serves to increase the lifetimes of neutrophil doublets formed through shear-induced two-body collisions. In turn, this would facilitate the engagement of more stable β_2 -integrin bonds and thus increase the two-body collision efficiency (fraction of collisions resulting in the formation of nonseparating doublets). To this end, suspensions of unstimulated neutrophils were subjected to a uniform shear field in a transparent counter-rotating cone and plate rheoscope, and the formation of doublets and growth of aggregates recorded using high-speed videomicroscopy. The dependence of neutrophil doublet lifetime and two-body collision-capture efficiency on shear rate, G , from 14 to 220 s^{-1} was investigated. Bond formation during a two-body collision was indicated by doublets rotating well past the orientation predicted for break-up of doublets of inert spheres. A striking dependence of doublet lifetime on shear rate was observed. At low shear ($G = 14 \text{ s}^{-1}$), no collision capture occurred, and doublet lifetimes were no different from those of neutrophils pretreated with a blocking antibody to L-selectin, or in Ca^{++} -depleted EDTA buffers. At $G \geq 66 \text{ s}^{-1}$, doublet lifetimes increased, with increasing G reaching values twice those for the L-selectin-blocked controls. This correlated with capture efficiencies in excess of 20%, and, at $G \geq 110 \text{ s}^{-1}$, led to the rapid formation of large aggregates, and this in the absence of exogenous chemotactic stimuli. Moreover, the aggregates almost completely broke up when the shear rate was reduced below 66 s^{-1} . Partial inhibition of aggregate formation was achieved by blocking β_2 -integrin receptors with antibody. By direct observation of the shear-induced interactions between neutrophils, these data reveal that steady application of a threshold level of shear rate is sufficient to support homotypic neutrophil aggregation.

INTRODUCTION

In response to inflammatory stimuli, neutrophils roll along post-capillary venular endothelium, and become firmly adherent before migrating out of the vascular space. Within the last decade, many of the biochemical and biophysical mechanisms underlying the recruitment of neutrophils by stimulated endothelium have been defined. Much of this knowledge has been obtained from experiments *in vitro*, using parallel-plate flow chambers and rotational viscometers. Experiments have revealed a multistep cascade of events beginning with margination and tethering of neutrophils to the wall of endothelium, progressing to transmembrane signaling and shear resistant adhesion (Springer, 1994; Vestweber and Blanks, 1999). Selectin–ligand bonds are involved in the rolling of leukocytes. It is generally accepted that these bonds have high mechanical strength, permitting tethering of the cell to the vessel wall through one or few bonds, and have fast on and off rates facilitating

rolling under hydrodynamic shear and normal forces (Jones et al., 1993; Alon et al., 1995; 1998; Finger et al., 1996). The transient tethering is thought to provide sufficient time for the β_2 (CD18) integrin family of neutrophil adhesion receptors to engage and form stronger bonds with their endothelial cell ligands, resulting in arrest of the neutrophils. These events occur at venular wall shear rates believed to vary from 150 to 1600 s^{-1} (Atherton and Born, 1973; von Andrian et al., 1992). Only at low shear rates, however, can the β_2 -integrin receptors by themselves mediate tethering and arrest of the neutrophils (von Andrian et al., 1992, 1993; Abassi et al., 1993; Jones et al., 1993; Hentzen et al., 2000).

In addition to heterotypic adhesion of neutrophils to endothelium, neutrophils engage in homotypic adhesion, whereby neutrophils flowing in the free stream are captured by those adherent to endothelium (Bargatze et al., 1994; Walchek et al., 1996). Homotypic adhesion (aggregation) of freely flowing neutrophils in sheared suspensions has also been extensively studied (Simon et al., 1990; Rochon and Frojmovic, 1991; Taylor et al., 1996; Neelamegham et al., 1997). One of us (S.I.S.), and others have shown that the receptor mechanisms underlying homotypic adhesion of neutrophils are analogous to those involved in heterotypic adhesion. Thus, adhesion of neutrophils to each other de-

Received for publication 5 April 2001 and in final form 21 June 2001.

Address reprint requests to Harry L. Goldsmith, University Medical Clinic, Montreal General Hospital, 1650 Cedar Avenue, Montreal, Quebec H3G 1A4, Canada. Tel.: 514-937-6011 x2920; Fax: 514-937-6961; E-mail: harry.goldsmith@mcgill.ca.

© 2001 by the Biophysical Society

0006-3495/01/10/2020/15 \$2.00

pend on L-selectin binding to its counter receptor P-selectin glycoprotein ligand-1 (PSGL-1) (Guyer et al., 1996; Taylor et al., 1996; Walchek et al., 1996), which leads to leukocyte function-associated antigen (CD11a/CD18) binding to intercellular adhesion molecule-3 (ICAM-3) (Okuyama et al., 1996; Neelamegham et al., 2000), and Mac-1 (CD11b/CD18) binding to an unknown receptor.

In the previous work (Taylor et al., 1996; Neelamegham et al., 1997), the aggregation of neutrophils activated with 1 μ M formyl peptide (formyl-methionyl-leucyl-phenylalanine; fMLP) and subjected to uniform shear in a cone and plate viscometer for various times was described. The reaction was then quenched with glutaraldehyde, and the distribution of single cells and aggregates of 2–6 cells determined using flow cytometry. It was found that the initial rate of aggregation increased with increasing shear rate from 100 to a maximum at 800 s^{-1} . The time-averaged collision capture efficiency, ε , was defined as the ratio of the number of collisions in the first 30 s resulting in the formation of aggregates to that of the total number of collisions, predicted by the Smoluchowski (von Smoluchowski, 1917) rectilinear two-body collision theory. It was shown that ε increased with increasing G up to a maximum at 400 s^{-1} , and that, at $G = 100$ and 200 s^{-1} , the collision efficiency doubled when the shear stress was doubled by increasing suspending medium viscosity through the addition of Ficoll. However, doubling the shear stress at $G > 400 s^{-1}$ significantly decreased the collision efficiency. The increase in ε with increasing G was found to be L-selectin-dependent: when L-selectin was blocked by the antibodies DREG-200 or lymphocyte adhesion molecule 1–3, β_2 -integrin-mediated aggregation was unchanged at $G = 100 s^{-1}$, whereas, at $G = 200$ and 400 s^{-1} , respectively, 70 and 95% of the aggregation was blocked.

One would have expected that, because the contact time between two colliding neutrophils decreases with increasing shear rate, and because there appears to be a requisite contact time for an integrin bond to form (Hentzen et al., 2000), the collision efficiency and degree of aggregation would decrease with increasing G . The results of Taylor et al. (1996) show that this is not the case, likely because of the formation of transient L-selectin bonds. Although their studies suggested that L-selectin functioned to prolong neutrophil contact and potentiate the engagement of β_2 -integrins over a relatively narrow range of shear rate and shear stress, the mechanism(s) remained unresolved.

The objective of the present work is to directly observe shear-induced two-body collisions between neutrophils in Couette flow to determine the roles of L-selectin and β_2 -integrin in the adhesion process. We have previously reported the use of a transparent counter-rotating cone and plate rheoscope to observe the shear-induced formation and break-up of doublets of sphered swollen red blood cells cross-linked by antibody (Tees et al., 1993), and of doublets of derivatized latex spheres covalently bearing receptor, cross-linked by

multi- or divalent ligand (Tees and Goldsmith, 1996; Kwong et al., 1996; Long et al., 1999). Here, we have used the rheoscope and high-speed videomicroscopy to plot the trajectories of colliding neutrophils and measure the times over which the cells are in apparent contact. We determined the effect of shear rate and shear stress on the collision efficiency, on the distribution of lifetimes of collision doublets, and on the rate of aggregation.

THEORETICAL CONSIDERATIONS

Two-body collision trajectories in shear flow

The fluid mechanical problem of predicting the trajectories of two interacting, neutrally buoyant, rigid spherical particles, radius b , in a simple shear flow has been solved (Batchelor and Green, 1972; Arp and Mason, 1977), and extended to the case when interaction forces, $F_{\text{int}}(h)$, other than hydrodynamic, operate at intersurface distances $h < 100$ nm (van de Ven and Mason, 1976; van de Ven, 1989). The relative velocity of the sphere centers a distance s apart, is given by

$$\frac{ds}{dt} = A(s^*)Gb \sin^2\theta_1 \sin 2\phi_1 + \frac{C(s^*)F_{\text{int}}(h)}{3\pi b\eta}, \quad (1)$$

and the angular motion of the doublet axis by

$$\frac{d\theta_1}{dt} = \frac{1}{4} B(s^*)G \sin 2\theta_1 \sin 2\phi_1, \quad (2)$$

$$\frac{d\phi_1}{dt} = \frac{1}{2} G[1 + B(s^*)\cos 2\phi_1]. \quad (3)$$

Here, θ_1 and ϕ_1 are the respective polar and azimuthal angles relative to X_1 as the polar axis, as shown in Fig. 1; $A(s^*)$ and $C(s^*)$ are known dimensionless functions of $s^* = s/b$, which have been documented (van de Ven and Mason, 1976; Arp and Mason, 1977). Eq. 3 describes the angular velocity of a rigid prolate ellipsoid of equivalent axis ratio r_e (Jeffery, 1922) with $B(s^*) = [r_e^2(s^*) - 1]/[r_e^2(s^*) + 1]$ applicable to a collision doublet of rigid spheres with $r_e = 1.98$ (Wakiya, 1971).

Rearrangement of Eq. 1 yields the force equation,

$$\frac{3\pi b\eta}{C(s^*)} \frac{ds}{dt} = \frac{A(s^*)}{C(s^*)} 3\pi\eta Gb^2 \sin^2\theta_1 \sin 2\phi_1 + F_{\text{int}}(h), \quad (4)$$

in which the term on the left represents the hydrodynamic drag force resisting approach of the particles, and the first term on the right the normal hydrodynamic force, F_n , between spheres acting along the line of their centers. When rotation occurs in the X_2X_3 plane, $\phi_1 = 90^\circ$, F_n is maximally compressive at $\phi_1 = -45^\circ$ and maximally tensile at $\phi_1 = +45^\circ$. For doublets of rigidly linked spheres, F_n has been computed (Tha and Goldsmith, 1986):

$$F_n = \alpha_n \eta Gb^2 \sin^2\theta_1 \sin 2\phi_1, \quad (5)$$

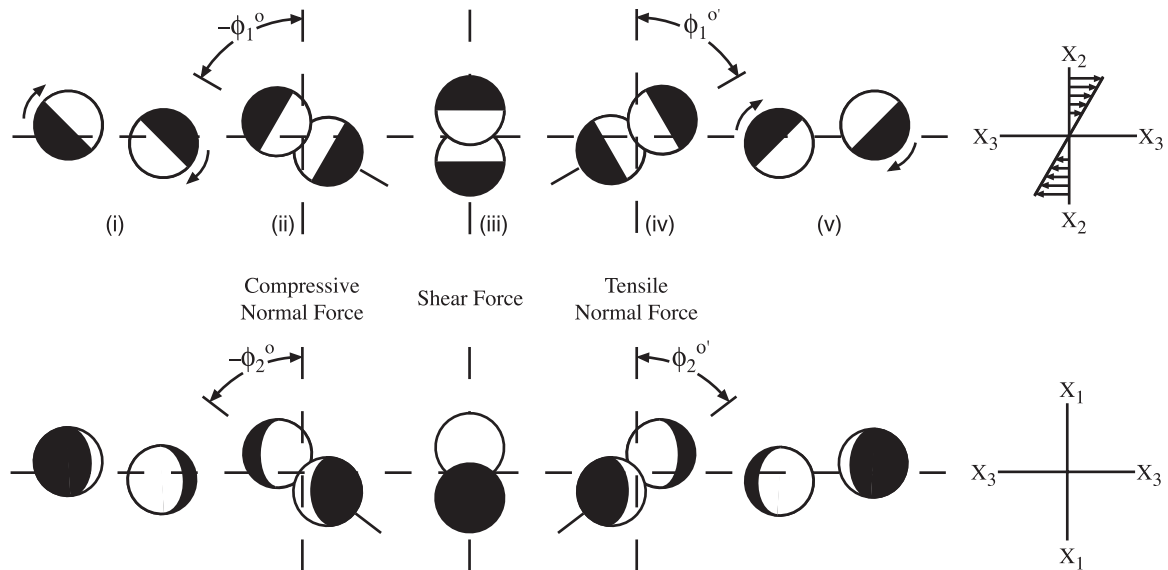


FIGURE 1 Two-body collisions between equal-sized noninteracting rigid spheres in Couette flow, as seen in the X_2X_3 plane (upper) and the X_1X_3 plane (lower): (i) approach; (ii) apparent contact at $\phi_1^0 = -60^\circ$ and $\phi_2^0 = -52.5^\circ$; (iii) mid-point of doublet rotation, when the normal compressive force is zero and the shear force is maximal; (iv) separation under tensile normal force at the mirror image angles $\phi_1^{0'} = +60^\circ$ and $\phi_2^{0'} = +52.5^\circ$; and (v) recession. The angles were computed assuming an orbit constant $C = 1.0$ (constant from integrated form of Eq. 2; adapted from Goldsmith and Mason, 1967).

where α_n is a force coefficient weakly dependent on h .

A collision, seen along the X_1 axis in the X_2X_3 plane is shown in the upper part of Fig. 1. In the rheoscope, collisions are viewed along the X_2 axis in the X_1X_3 plane, as shown in the lower part of Fig. 1. As seen under the microscope, the spheres make apparent contact at $\phi_1 = -\phi_1^0$ and $\phi_2 = -\phi_2^0$, as the normal compressive hydrodynamic force acting along the axis brings their surfaces to within distances of $h < 50$ nm of each other. As the doublet axis rotates past the orientation $\phi_1 = \phi_2 = 0$, perpendicular to the flow, the normal force becomes tensile and h increases, until the point of apparent separation, at $\phi_1 = \phi_1^{0'}$ and $\phi_2 = \phi_2^{0'}$. Such doublets are defined as transient, as opposed to those defined as nonseparating, in which the spheres have been captured, as described below. In the absence of interaction forces, $F_{\text{int}}(h)$, other than hydrodynamic, the trajectory of approach is a mirror image of the trajectory of separation ($ds/dt_{\text{approach}} = ds/dt_{\text{separation}}$), hence $|\phi_1^0| = |\phi_1^{0'}|$ and $|\phi_2^0| = |\phi_2^{0'}|$.

Although passive neutrophils are spherical, their surfaces are highly ruffled, due to excess membrane forming many folds, projections, and microvilli on the surface of the cells (average static lengths $\sim 0.3 \mu\text{m}$; Shao et al., 1998). The ruffles may affect the trajectories of two approaching neutrophils in shear flow, in that the centers of colliding neutrophils may not be able to approach as close to each other as the centers of colliding smooth rigid spheres. The result would be a more rapid separation of sphere centers, so that $ds/dt_{\text{separation}} > ds/dt_{\text{approach}}$, as if they had repelled each other. Even in the case of “smooth” latex spheres, such

apparent repulsion, possibly due to surface asperities of the spheres or solvation forces, has been described (Takamura et al., 1981a). Similarly, repulsion was observed in two-body collisions between sphered, glutaraldehyde-fixed erythrocytes (Goldsmith et al., 1981). Thus, in the absence of adhesive interactions such as bond formation, or compression of the neutrophil membrane during collision, it is expected that $|\phi_1^{0'}| < |\phi_1^0|$. As a consequence, the measured mean doublet lifetime, $\langle \tau_{\text{meas}} \rangle$, would be less than the theoretical one, $\langle \tau_{\text{theor}} \rangle = 5\pi/6G$ (Bartok and Mason, 1957).

Two-body collision capture efficiencies

Traditionally, the two-body collision frequency per unit volume of a sheared suspension containing N singlets ml^{-1} , J , has been computed assuming, as originally done by Smoluchowski (1917), that all particles move along linear trajectories until they collide with a sphere. The classical theory has been corrected using the rigorous hydrodynamic theory of curvilinear particle collision trajectories described by Eq. 1 with $F_{\text{int}}(h) = 0$ (Arp and Mason, 1976) and extended to the case when $F_{\text{int}}(h) \neq 0$, taking into account the electrostatic repulsion and van der Waals attraction between colloidal size charged smooth spheres. It has been applied to latex spheres (van de Ven, 1989), and to platelets and neutrophils (Tandon and Diamond, 1997; 1998), assumed to be spherical.

When interparticle forces act between the spheres, the collision capture frequency per particle, J_c , giving the num-

number of collisions that result in nonseparating doublet formation, assuming rectilinear approach, is given by

$$J_c = \varepsilon \frac{16}{3} N^2 G b^3, \quad (6)$$

where $\varepsilon = J_c/J$ is the two-body collision capture efficiency.

Capture efficiencies have also been computed using rigorous hydrodynamic theory (van de Ven and Mason, 1977) and ε given as a function of the ratios of the repulsive and attractive forces to the hydrodynamic force. In the absence of repulsive forces, for equal-sized spheres, ε decreases with increasing G , as would be expected from Eq. 4, because, with increasing G , both the hydrodynamic drag and the hydrodynamic normal force between spheres increase while the interaction force remains constant. When both repulsive and van der Waals forces act, ε is predicted to first increase at low G , then to decrease at moderate and high G , as confirmed by a number of studies in sheared suspensions of charged latex spheres (Swift and Friedlander, 1964; Curtis and Hocking, 1970; van de Ven and Mason, 1977).

However, as pointed out in the Introduction, in the case of activated neutrophils in the range $100 \leq G \leq 400 \text{ s}^{-1}$, ε and the degree of aggregation actually increase with increasing G , due to the formation of transient L-selectin bonds (Taylor et al., 1996). Their results have been modeled with the aid of two-body hydrodynamic collision theory (Tandon and Diamond, 1998). The model predicts that colliding neutrophils initially bridged by at least one L-selectin–PSGL-1 bond require a lifetime of 52.5 ms at $G \geq 400 \text{ s}^{-1}$ to subsequently become a stable aggregate. That time is $\sim 1.3 \times$ the period of rotation, T , of rigidly linked doublets of spheres ($T = 15.62/G$; Wakiya, 1971), and $\sim 8 \times$ the predicted mean collision doublet lifetime $\langle \tau_{\text{theor}} \rangle$.

MATERIALS AND METHODS

Reagents

Hydroxy ethyl-cellulose (HEC, middle viscosity 1) was purchased from Fluka Chemie (Buchs, Switzerland), fMLP and human serum albumin from Sigma-Aldrich Canada (Oakville, ON, Canada). Percoll and Ficoll 400 were purchased from Amersham Pharmacia Biotech AB (Uppsala, Sweden). Fluorescein isothiocyanate (FITC)-labeled MAb DREG 56 was obtained from Immunotech (Marseilles, France). Protein Design Labs (Mountain View, CA) kindly supplied a humanized DREG. Fab fragments of MoAb LAM1-3 (Cell Genesys, Foster City, CA) were produced by digestion with papain and purified by passage over a protein-A-Sepharose column (Taylor et al., 1996) using an ImmunoPure Fab preparation kit from Pierce (Rockford, IL). Dr. Robert Rothlein at Boehringer-Ingelheim Pharmaceuticals (Ridgefield, CT) generously provided the R15.7 antibody to β_2 -integrin.

Isolation of neutrophils

Human neutrophils were prepared as previously described by Rochon and Frojmovic (1991). Thirty milliliters of blood was collected from healthy subjects (3 female, 4 male donors) by venipuncture with a butterfly-19

needle (1 vol citrate:9 vol whole blood). One percent HEC at 37°C was then added and gently mixed with the citrated blood in a polypropylene tube (1 vol HEC:4 vol citrated WB) to aggregate the red cells. The layer of supernatant leukocyte rich plasma (from 17 to 20 ml) was extracted, layered over 20 ml of 54% isotonic Percoll ($1.076 \text{ g} \cdot \text{ml}^{-1}$) in a 50-ml polypropylene tube and centrifuged at $500 \times g$ at 4°C for 20 min. Four milliliters ice cold H_2O was added to the red blood cell neutrophil pellet and gently mixed for 20 s to hemolyse the red blood cells, and then rapidly pipetted into $\text{Ca}^{++}/\text{Mg}^{++}$ -free Tyrodes (pH = 7.4; concentration in mmol l^{-1} : NaCl, 136; KCl, 2.7; NaHCO_3 , 11.9; NaH_2PO_4 , 0.36; glucose, 5.6) to a final volume of 30 ml to restore salt concentration to isotonic values. Finally, the suspension was centrifuged at $100 \times g$ at 4°C for 8 min and the pellet of neutrophils resuspended into 0.3–0.5 ml $\text{Ca}^{++}/\text{Mg}^{++}$ -free Tyrodes containing 0.25% HSA. This suspension was kept on ice during the experiment. The number concentration of cells was obtained by counting aliquots diluted $5 \times$ with a 5% acetic acid solution of crystal violet using a hemocytometer.

It should be noted that the above isolation of neutrophils involves a two-step centrifugation procedure unlike the isolation method of Simon et al. (1995) used in the previous papers, involving one-step sedimentation through a Ficoll-hypaque density gradient. Nevertheless, the appearance of the cells under a high power microscope in the present experiments, their exclusion of trypan blue (>98%), and maintenance of >90% membrane-bound L-selectin over 2 h on ice, is evidence that there were no obvious signs of cell deterioration or activation. Shearing of neutrophil suspensions in the rheoscope could be carried out up to 2 h after isolation of the neutrophils, at which time the cells began to change shape and pseudopods began to develop.

Flow cytometry

The presence of membrane-bound L-selectin was used to determine the state of activation of the neutrophils, as reported by FITC-labeled MAb DREG 56. Twenty-microliter aliquots of a suspension, containing 5000 cells $\cdot \mu\text{l}^{-1}$ in phosphate-buffered saline containing 2 mM Ca^{++} , were mixed with FITC-labeled DREG 56. After incubation with ligand for 30 min in the dark, the reaction was quenched by diluting the cell suspension with 10 volumes of FACSFlow (Becton Dickinson Canada, Mississauga, ON, Canada). 3000 particles were counted in a FACSCaliber flow cytometer (Becton Dickinson Canada, Mississauga, ON, Canada), within 30–60 s to minimize post-dilution time-dependent changes. Mean fluorescence values associated with FITC-DREG 56 binding to L-selectin on the neutrophils were compared with those obtained in the presence of 500 nM fMLP, which caused the neutrophils to shed L-selectin. The neutrophils kept on ice in Tyrodes-albumin were found to have >90% L-selectin expressed on their surface over a period of >2 h after isolation from blood, whereas those activated with fMLP expressed <3% L-selectin.

Rheoscope

Two-body collisions between neutrophils in Couette flow were observed and videotaped in a transparent counter-rotating cone and plate rheoscope (model MR-1, Myrenne Instruments, Fremont, CA) with a nominal cone angle $\psi = 2^\circ$, mounted on a specially constructed stage on a Zeiss Axiovert inverted microscope (Carl Zeiss Ltd., Montreal, QC, Canada). Using a 10-turn variable resistor, the rheoscope cone and plate angular velocities, Ω , and the shear rate, $G = 2\Omega/\tan \psi$, was varied 14–220 s^{-1} . The actual value of the cone angle ($2^\circ \pm 0.03^\circ$) was checked under a microscope at $500 \times$ magnification. As well, the radius, d , of a central area of flattening (up to $\sim 0.2 \text{ mm}$), which developed with use, was measured. When flattening is considered, $G = (2\Omega/\tan \psi)[1 + d/(R - d)]$, where R is the distance from the cone center.

Videotaping neutrophil interactions

Ten microliters of the neutrophil suspension on ice was added to 40 μl of 12.5% or 6.25% Ficoll 400 containing 0.8 mM MgCl_2 and 1.8 mM CaCl_2 , and gently mixed. Thirty-microliters of this suspension, containing between 15,000 and 25,000 neutrophils/ μl was allowed a minute to warm up to room temperature (22°C), before pipetting it onto the plate of the rheoscope. The microscope was focused on the layer of zero translational velocity located in the mid-plane of the gap, at a distance 1.15 mm from the center of the cone corresponding to a vertical distance $\Delta X_2 = 36.7 \mu\text{m}$ ($d = 0.2 \text{ mm}$) between cone and plate surfaces. The neutrophil trajectories and the formation of aggregates were observed using a 16 \times objective and recorded using a high-speed digital camera (KODAK Motion Corder Analyzer, model SR-500c, Roper Scientific MASD, San Diego, CA) capable of storing 1364 frames in a given sequence. Sequences were videotaped over 22.5 and 10.8 s at shear rates of 14 and 32 s^{-1} and framing rates of 60 and 125 s^{-1} , respectively. At $G = 66$ and 110 s^{-1} , sequences were videotaped over 5.4 s and framing rates of 250 s^{-1} , and at $G = 220 \text{ s}^{-1}$ also over 5.4 s at a framing rate of 500 s^{-1} , but at half frame. Using a cone and plate digital viscometer, (Brookfield Engineering Laboratories, Can-Am Instruments, Mississauga, ON, Canada), suspending phase viscosities of 10.0 and 5.0% buffered Ficoll were 5.49 ± 0.48 (SD, $n = 36$) and 2.76 ± 0.18 ($n = 4$) mPa s (22°C), respectively, and the densities were 1.035 and 1.016 g ml^{-1} , respectively. Given the mean diameters of a population of neutrophils in buffered Ficoll = $8.71 \pm 0.42 \mu\text{m}$ ($n = 25$), the sedimentation rates were estimated to be 0.38 and 1.04 $\mu\text{m s}^{-1}$, respectively. Thus, it would take 48 and 18 s in 10 and 5% buffered Ficoll, respectively, for a cell suspended in the mid-plane to settle onto the plate of the rheoscope. It was found that between 10 and 20 two-body collisions between freely suspended cells could be recorded in a sequence.

The data obtained was then downloaded onto videotape (model ST-120, Panasonic, Osaka, Japan) at 30 frames s^{-1} , for subsequent analysis.

Data Analysis

Two-body collisions

The videotape sequences were searched for all apparent collisions that occurred between neutrophils. When an apparent collision was found, the velocities of both neutrophils involved were determined using a video position analyzer (model VPA-1000, FOR-A Co., Ltd., Tokyo, Japan), to ensure that one or both cells were not rolling on the rheoscope plate, and that the relative particle translational velocities, $\Delta u_3 \leq \Delta u_{3\text{max}} = 2Gb$, the maximum value corresponding to sphere center separations of one cell diameter = $2b$.

The X_3 and X_1 coordinates of the centers of the two cells of a doublet were recorded before, during and after colliding, and ϕ_2 computed from

$$\phi_2 = \tan^{-1} \left(\frac{X_3^1 - X_3^2}{X_1^1 - X_1^2} \right), \quad (7)$$

where the superscripts refer to cells 1 and 2 of the doublet. Of particular interest are the values of $\Delta\phi_2 = |\phi_2^0| - |-\phi_2^0|$, because positive values may indicate the temporary formation of a bond(s) between the colliding cells. If such bonds persisted throughout the quadrant $0 < \phi_1 < 90^\circ$ in which F_n was tensile, and past the orientation $\phi_1 = 90^\circ$ ($\phi_2 = \phi_{2\text{max}}$; Tees et al., 1993) when the doublet was aligned with the direction flow, the cells were considered as having been captured, and counted as nonseparating doublets. The collision capture efficiency ε was then computed by dividing the number of doublets that rotated past $\phi_1 = 90^\circ$, by the total number of two-body collisions analyzed. Such “nonseparating” collision doublets were followed until they broke-up or disappeared from view, and if broken up, the time of separation recorded.

Rates of aggregation and disaggregation

The rates of formation of nonseparating doublets, triplets, and higher-order multiplets in neutrophil suspensions were videotaped over 22.5 s at $G = 66$ and 110 s^{-1} at a framing rate of 60 s^{-1} , and over 10.8 s at $G = 220 \text{ s}^{-1}$ at a framing rate of 125 s^{-1} . Beginning at the instant of the application of shear, frames were chosen at suitable intervals of time and the number of singlets and aggregates counted. Singlets and aggregates, the latter binned into doublets and triplets, and all higher-order multiplets were counted. The mean and SEM of values from 5 sequences were computed. To ensure that no transient aggregates were counted, particles were observed over several frames before and after the one being analyzed.

To obtain the rates of disaggregation, suspensions of neutrophils were first allowed to aggregate for a period of 10 s while applying shear at $G = 110$ or 220 s^{-1} . Videorecording commenced at $t = 9$ s, and a second later, the shear rate reduced as rapidly as possible by turning down the rheoscope variable resistor to the position corresponding to $G = 14 \text{ s}^{-1}$, a process which took ~ 2.5 s from $G = 110 \text{ s}^{-1}$ and ~ 4.5 s from $G = 220 \text{ s}^{-1}$.

Error analysis

Viscosity: Temperature fluctuation of $\pm 0.2^\circ\text{C}$ over the course of an experiment would result in an error of ± 4 –7% in the viscosity, and hence in the computed shear stress.

Angle difference $\Delta\phi_2$: The error in the measurement of X_1 and X_3 (Eq. 7) was one pixel = 1.28 μm , resulting in errors of $\pm 4^\circ$ in $\Delta\phi_2$.

Doublet lifetime: An error of one frame appears reasonable in the observer’s judgment of the time elapsed between initial apparent contact and separation of the spheres. This corresponds to an error in the mean measured lifetimes, which increased from 2 in 15 frames or $\pm 13\%$ at $G = 66 \text{ s}^{-1}$ to 1 in 12.5 frames, or $\pm 16\%$ at $G = 220 \text{ s}^{-1}$.

RESULTS

The most striking result was the effect of increasing G on the number of nonseparating collision doublets and subsequent formation of multicellular aggregates. At $G = 14$ and 32 s^{-1} , a significant fraction of transient doublets continued to rotate past the mirror image of the apparent angle of approach, $\Delta\phi_2 > 0$, but very few nonseparating doublets were seen. However, at $G \geq 66 \text{ s}^{-1}$, the tendency for stable adhesion increased markedly, as a significant number of nonseparating collision doublets were observed. Moreover, at $G = 110$ and 220 s^{-1} , there was a rapid formation, within 2 s of the onset of shear, of aggregates consisting of more than 5 neutrophils. By 5 s of shear at high G , some of these aggregates had grown to particles > 15 cells, accompanied by a large decrease in the numbers of singlets. The largest aggregates were elliptical in shape; linear aggregates were rarely seen. The aggregation was shown to be reversible: as the shear rate was reduced below 66 s^{-1} , the larger aggregates quickly began to break up, and finally when it was lowered to 14 s^{-1} , all triplets and higher-order multiplets disappeared and the collision capture frequency was essentially zero. The largest elliptical aggregates first broke up into 3 or 4 smaller rounded aggregates, which then quickly broke up into triplets and doublets.

That L-selectin on the neutrophil was involved in homotypic neutrophil adhesion was shown by pre-incubating the

cells for 15 min with either an Fab fragment of anti L-selectin (LAM 1–3) or the monoclonal antibody CD62L (DREG-56), before subjecting them to shear in the rheoscope. These blocking antibodies effectively, but not completely, suppressed the formation of aggregates at high shear rate, leaving only doublets and triplets of cells. The involvement of β_2 -integrins in aggregation was examined by pre-incubating the neutrophils with anti-CD18 (R15.7). This treatment significantly inhibited the formation of the larger aggregates at high shear rate, but left intact the fractions of doublets and triplets. Depletion of extracellular Ca^{2+} by pre-incubating suspensions with a 2-mM EDTA buffer, virtually eliminated nonseparating doublets and blocked aggregation at all shear rates.

Effect of shear rate on doublet lifetimes and collision efficiency

The difference between the rotation of a transient and nonseparating collision doublet is illustrated by plots of the time course of the ϕ_2 orientation of the doublet axes shown in Fig. 2. In the case of the transient doublet (Fig. 2a), separation of the cells was observed at $\Delta\phi_2 > 0$ ($=20.7^\circ$), whereas in the case of the nonseparating doublet (Fig. 2b) rotation continued through one more half orbit (through $\phi_1 = 180^\circ$) before the spheres separated.

The data on doublet lifetimes are given in Table 1, presenting the mean measured lifetimes ($\langle\tau_{\text{meas}}\rangle \pm \text{SEM}$) of the collision doublets, and compared to those predicted ($\langle\tau_{\text{theor}}\rangle$) at each shear rate. Table 2 presents the measured time average collision capture efficiencies, ε , and the fractions of transient and nonseparating doublets. Based on rectilinear approach of sphere centers, τ_{theor} is given by

$$\tau_{\text{theor}} = \frac{5}{G} [\tan^{-1}(0.5 \tan \phi_1^0)]. \quad (8)$$

For glancing collisions at $\phi_1^0 = 5^\circ$, τ_{theor} has a value only $1/2$ of the mean collision doublet lifetime, whereas for near head-on collisions at $\phi_1^0 = 85^\circ$ $\tau_{\text{theor}} = 2.65\langle\tau_{\text{theor}}\rangle$; at $\phi_1^0 = 50^\circ$, $\tau_{\text{theor}} = \langle\tau_{\text{theor}}\rangle$. Yet the collision frequency, a function of the relative velocities of the spheres, Δu_3 , in turn a function of sphere center separation along the X_2 -axis (Fig. 1), is high at $\phi_1^0 = 5^\circ$, $\Delta u_3 = 0.962\Delta u_{3\text{max}}$, and low at $\phi_1^0 = 85^\circ$, $\Delta u_3 = 0.086\Delta u_{3\text{max}}$. Measurements of $\Delta u_3/\Delta u_{3\text{max}}$ at $G = 110 \text{ s}^{-1}$ for over 300 collision doublets binned into 5 intervals of $\Delta u_3/\Delta u_{3\text{max}} = 0.2$, showed that neutrophil flux at low ϕ_1^0 had been well sampled: 27.5% of all collision doublets analyzed lay in the bin $0.8 \leq \Delta u_3/\Delta u_{3\text{max}} \leq 1.0$, corresponding to the highest collision frequencies. The values of $\Delta u_3/\Delta u_{3\text{max}}$ then decreased to 26.2%, 24.8%, 19.1% and 3.0% in the succeeding 4 bins.

It is evident that there is a steady increase in the ratio $\langle\tau_{\text{meas}}\rangle/\langle\tau_{\text{theor}}\rangle$ with increasing shear rate, from ~ 1.0 at $G = 14 \text{ s}^{-1}$ until, at $G = 110$ and 220 s^{-1} , it is greater than

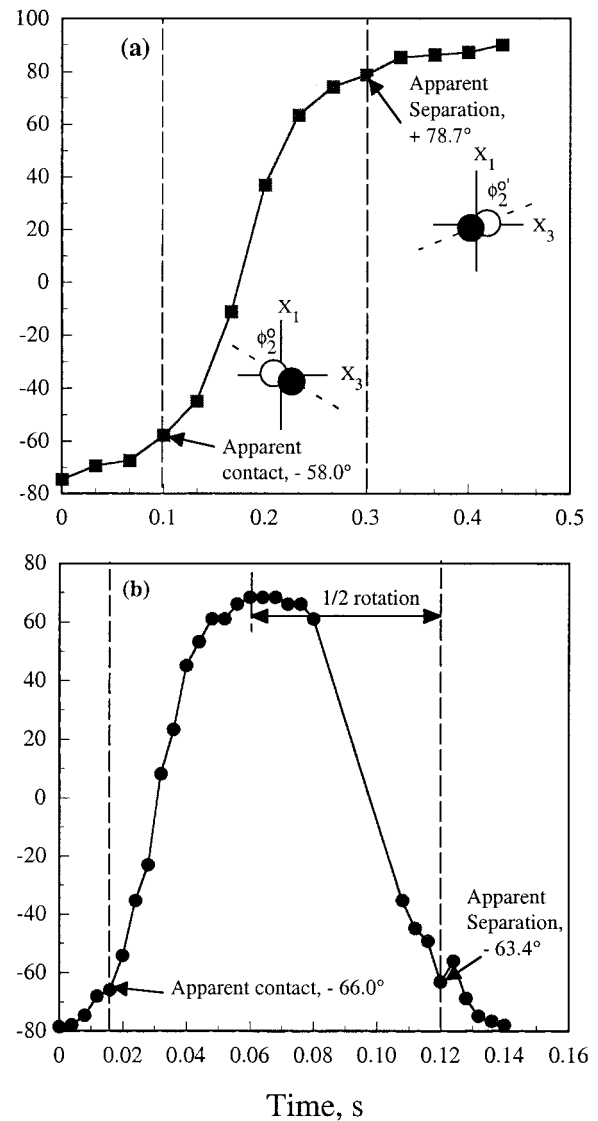


FIGURE 2 Plot of the measured ϕ_2 orientation of the axes of neutrophil collision doublets. (a) Transient doublet at $G = 14 \text{ s}^{-1}$ in which the cells were in apparent contact over 0.2 s (between the dashed lines) and $\phi_2 > 0$. (b) Nonseparating doublet at $G = 110 \text{ s}^{-1}$: Collision resulting in a doublet in which the neutrophils were captured and rotated together for a further half orbit before breaking up.

double that predicted. By contrast, in the Ca^{++} -depleted or L-selectin-blocked cell suspensions at $G = 110$ and 220 s^{-1} , only 5 of over 500 doublets were nonseparating and the mean $\langle\tau_{\text{meas}}\rangle/\langle\tau_{\text{theor}}\rangle$ were unity. The data in Table 2 show that $\varepsilon = 0$ at $G = 14 \text{ s}^{-1}$, thereafter increasing with increasing shear rate to 0.294 at $G = 110 \text{ s}^{-1}$ and decreasing to 0.206 at $G = 220 \text{ s}^{-1}$, even though $\langle\tau_{\text{meas}}\rangle/\langle\tau_{\text{theor}}\rangle$ is the highest at this shear rate. The increase in ε was accompanied by a decrease in the fraction of transient doublets having $\Delta\phi_2 < 0$, and by the appearance of increasing numbers of nonseparating doublets. As shown in Fig. 3 at $G = 110 \text{ s}^{-1}$, there was a fairly wide spread in the distri-

TABLE 1 Effect of shear rate on mean collision doublet lifetime

Number of Doublets	Shear Rate (s^{-1})	Framing Rate (s^{-1})	Mean Doublet Lifetime (s)		$\frac{\langle \tau_{\text{meas}} \rangle}{\langle \tau_{\text{theor}} \rangle}$
			Measured \pm SEM	Theoretical*	
63	14	60	0.183 ± 0.007	0.187	0.98
120 [†]	14	60	0.234 ± 0.010	0.187	1.25
98	32	125	0.096 ± 0.007	0.082	1.17
88	66	250	0.060 ± 0.005	0.040	1.50
251	110	250	0.050 ± 0.005	0.024	2.08
128 [‡]	110	250	0.037 ± 0.005	0.024	1.42
92	220	250	0.025 ± 0.007	0.012	2.08
Controls: 2mM EDTA					
307	110	250	0.026 ± 0.001	0.024	1.08
109	220	250	0.014 ± 0.001	0.012	1.17
Controls: anti-L-selectin					
95	110	250	0.024 ± 0.001	0.024	1.00

10% Ficoll in Tyrodes; $\eta = 5.49$ mPa s

* $\langle \tau_{\text{theor}} \rangle = 5\pi/6G$

[†]Pre-incubated for 3 min with 200 pM fMLP.

[‡]5% Ficoll in Tyrodes, $\eta = 2.7$ mPa s

bution in $\Delta\phi_2$ for the transient doublets; 74% of doublets had $\Delta\phi_2$ between -20° and $+20^\circ$. The mean value was $\Delta\phi_2 = -0.06^\circ \pm 10.50^\circ$ (SD).

It should be noted that the values of τ_{meas} could only include those nonseparating doublets that were seen to break up before disappearing from view ($<30\%$ at $G \geq 66$ s^{-1}), whereas the values of ε in Table 2 included all nonseparating doublets, hence the number of doublets are greater than in Table 1. Therefore, we carried out further experiments at $G = 110$ s^{-1} in which the number of observable doublet rotations in each sequence was significantly increased by reducing both the magnification and camera framing rate. As shown in Fig. 4, the distribution of $\tau_{\text{meas}}/\langle \tau_{\text{theor}} \rangle$ of nonseparating doublets varied from 6.04 to

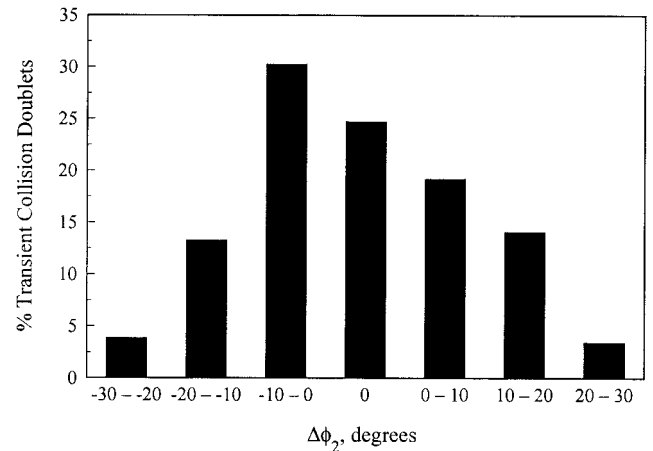


FIGURE 3 Histogram of the differential distribution in $\Delta\phi_2$ of transient collision doublets at $G = 110$ s^{-1} binned into intervals of 10° , $N = 303$. 74% of the doublets lie in the interval $-30^\circ < \Delta\phi_2 < +30^\circ$.

>49 with 71% having $\tau_{\text{meas}}/\langle \tau_{\text{theor}} \rangle$ greater than 6.04. The average lifetime and $\langle \tau_{\text{meas}} \rangle/\langle \tau_{\text{theor}} \rangle$ of 74 nonseparating doublets was 0.378 $s \pm 0.035$ and 15.87 ± 1.45 , respectively, corresponding to an average of 2.75 ± 0.53 rotational orbits. We estimate that the value of $\langle \tau_{\text{meas}} \rangle/\langle \tau_{\text{theor}} \rangle = 2.08$ shown in Table 1 for 251 doublets should in fact be closer to 6.2 by including the above ratio of 15.87 as the average for the 106 doublets (Table 2) lost to view before break-up.

Finally, it should be emphasized that the measured collision efficiencies are based on the observed two-body collisions between single neutrophils over a period of 5 s at $G = 110$ and 220 s^{-1} . However, as shown below, at these shear rates, a significant fraction of the total neutrophils are already present as aggregates within 2 s of the onset of shear.

TABLE 2 Effect of shear rate on $\Delta\phi_2$ and collision capture efficiency

Number of Doublets	Shear Rate (s^{-1})	Fraction of all Doublets that were Transient		Fraction of Nonseparating Doublets		Collision Efficiency ε
		$\Delta\phi_2 \leq 0$	$\Delta\phi_2 > 0$	broke up after 1 to 5 rotations	no break-up before lost to view	
63	14	0.452	0.548	0	0	0
131*	14	0.465	0.473	0	0.061	0.061
104	32	0.404	0.519	0	0.057	0.057
106	66	0.330	0.443	0.066	0.160	0.226
357	110	0.336	0.370	0.062	0.232	0.294
140 [†]	110	0.386	0.400	0.078	0.136	0.214
112	220	0.473	0.321	0.027	0.179	0.206
Controls: 2 mM EDTA						
307	110	0.488	0.505	0.007	0	0.007
109	220	0.615	0.385	0	0	0
Controls: anti-L-selectin						
100	110	0.370	0.600	0.030	0	0.030

10% Ficoll in Tyrodes; $\eta = 5.49$ mPa s

*Pre-incubated for 3 min with 200 pM fMLP

[†]5% Ficoll, $\eta = 2.7$ mPa s

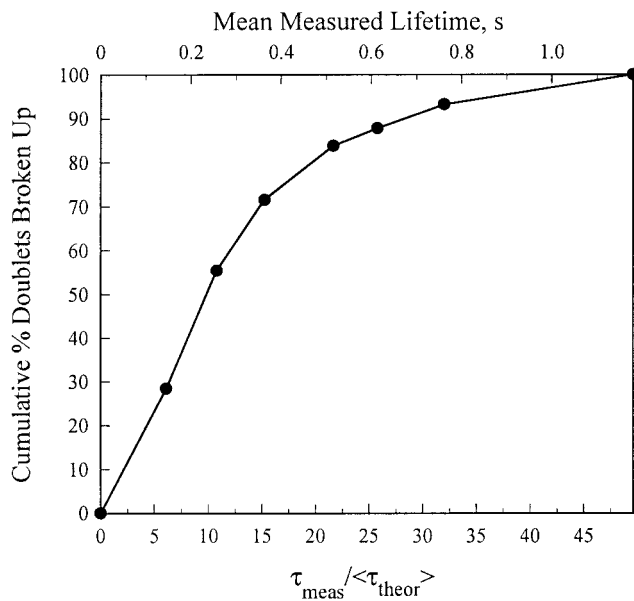


FIGURE 4 Distribution of lifetimes of nonseparating doublets at $G = 110 \text{ s}^{-1}$ when the observable number of doublet rotations was significantly increased by lowering magnification and filming rate (60 frames/s). Plot of the cumulative percent break up of doublets as a function of lifetime (*upper abscissa*) and ratio $\tau_{\text{meas}}/\langle\tau_{\text{theor}}\rangle$ (*lower abscissa*). The data are based on 74 doublets, of which 72 broke up over a range of additional rotational orbits from $\frac{1}{2}$ to 7, after remaining intact in the quadrant $0 \leq \phi_1 \leq 90^\circ$. Two doublets rotated for 10 and 14.5 orbits, respectively.

Rates of aggregation

Effect of shear rate

Aggregation, defined as the ratio of the number of neutrophils in aggregates/total number of neutrophils observed, is plotted in Fig. 5 *a* at $G = 66, 110$ and 220 s^{-1} over the first 18 s of shear. Both the rate and extent of aggregate formation increased markedly with increasing shear rate. The initial rates increased from 4.6 to 6.4 to $23.9\% \text{ s}^{-1}$ at 66, 110, and 220 s^{-1} , respectively, and the mean maximum extent of aggregation increased from 13.3 to 52.6 to 80.5%, respectively. The maximum was reached between 6 and 10 s and remained constant up to 1 min (not shown; the mean measured values between 50 and 62-s shear were 13.6, 52.6, and 82.1%, respectively).

However, these plots do not show the accompanying growth in aggregate size, which is illustrated in the histograms on the left in Fig. 6 presenting the fraction of neutrophils in singlets, doublets, and triplets, and all higher-order multiplets at their maximum, after 10.8 s of shear. There was a marked increase in aggregate growth in going from $G = 66 \text{ s}^{-1}$, where almost no multiplets were present, to $G = 110 \text{ s}^{-1}$, when the mean fraction of cells in multiplets ($\sim 29\%$) exceeded that in doublets and triplets ($\sim 20\%$). After 60 s of shear, these fractions were reversed because some of the higher-order aggregates had broken up into doublets and triplets (not shown). At $G = 220 \text{ s}^{-1}$,

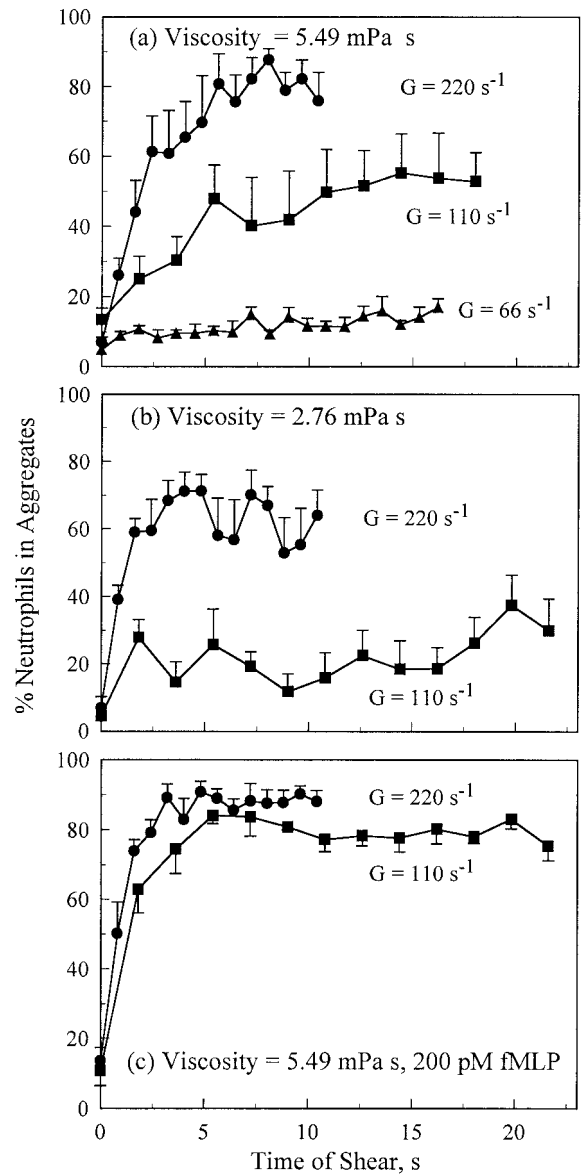


FIGURE 5 Effect of shear rate and shear stress on the rate of neutrophil aggregation in (a) 10% Ficoll at $G = 66, 110$, and 220 s^{-1} ; (b) 5% Ficoll at $G = 110$ and 220 s^{-1} ; (c) 10% Ficoll with neutrophils preincubated for 3 min with 200 pM fMLP. Plot of the mean fraction of neutrophils in aggregates ($\pm \text{SEM}$, $n = 5$) against time of shear. There was a marked rise in the rate and extent of aggregation with increasing shear rate and a significant reduction in the extent of aggregation in 5% Ficoll at the lower shear stress. The chemotactically stimulated cells exhibited a significant increase in the rate and extent of aggregation.

$>70\%$ of neutrophils were found in multiplets between 5 and 10 s of shear; that fraction then slowly decreased to 57% at 60 s of shear (not shown).

Fragmentation of aggregates

The fact that the extent of aggregation was found to reach a steady state with $<100\%$ neutrophils in aggregates after

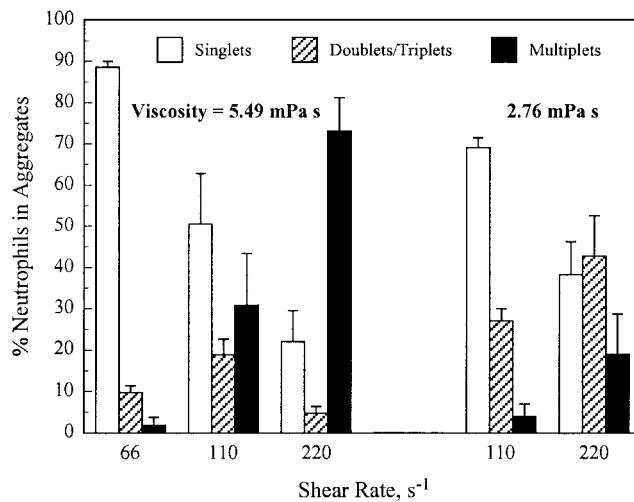


FIGURE 6 Effect of shear rate and shear stress on the distribution of aggregate size after 10.8 s of shear. Data from Fig. 5, *A* and *B*, showing histograms of the mean fraction of neutrophils binned into singlets, doublets and triplets, and higher-order multiplets. *Left*: 10% Ficoll, $\eta = 5.49$ mPa s; *Right*: 5% Ficoll, $\eta = 2.76$ mPa s, showing the marked effect of shear rate and shear stress on aggregate size.

10 s of shear implied that either fragmentation and reaggregation were occurring, or that there was a population of neutrophils that did not aggregate. Analysis of the experiments at $G = 110$ s⁻¹ in the time intervals $10 < t < 20$ s and $50 < t < 60$ s clearly showed that the former mechanism was at work. The fraction of all aggregates that were seen to fragment was found to be somewhat greater after 50 s than after 10 s of shear, 69.0% ($n = 126$) and 59.0% ($n = 268$), respectively. Overall, the most frequent mode of fragmentation was by loss of a single neutrophil: 65.2 and 74.7% of all aggregates fragmented in this way after 10 and 50 s, respectively. As expected, the fraction of aggregates that fragmented by loss of 2 or more cells increased with aggregate size. Thus, 19, 36, 50, and 63% of aggregates of 4–5, 6–7, 8–10, and >10 cells, respectively, fragmented by loss of 2 or more cells in the 10–20 s time interval.

Effect of shear stress

The effect of shear stress on doublet lifetime and collision efficiency at $G = 110$ s⁻¹, and on aggregation at $G = 110$ and 220 s⁻¹ was studied by suspending the cells in 5% buffered Ficoll, thereby reducing the shear stress from 0.60 to 0.30 Pa at $G = 110$ s⁻¹ and from 1.21 to 0.61 Pa at $G = 220$ s⁻¹. The results from Tables 1 and 2 show that, at $G = 110$ s⁻¹, the mean doublet lifetime decreased by 9.2% and the collision efficiency by 27% from the values at the higher shear stress.

The effect of decreasing the shear stress on the rate and extent of aggregation is shown in Fig. 5 *b* and on the right in Fig. 6. Although the initial rate of aggregation at $G = 220$

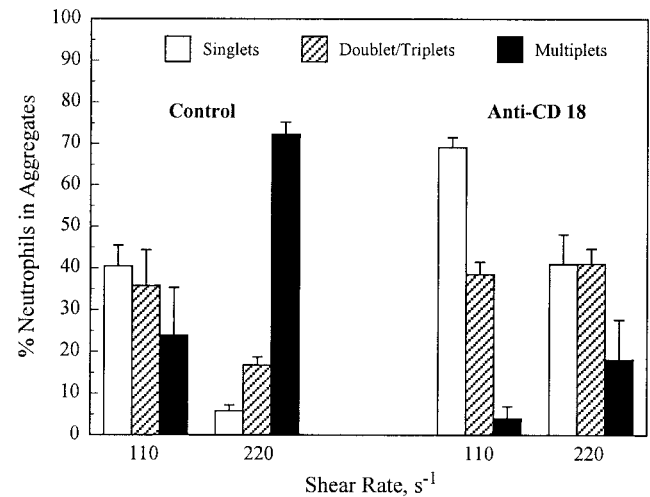


FIGURE 7 Effect of pre-incubation of neutrophils with anti-CD18 (monoclonal antibody R15.7) on the distribution of aggregate size after 10.8 s of shear. Histograms, as in Fig. 6, of the percent neutrophils in singlets and in aggregates, binned into doublets and triplets, and higher-order multiplets. *Left*: Neutrophils incubated at room temperature for 5 min before shear without addition of antibody. *Right*: Neutrophils incubated for 5 min with 10 μ g/ml of R15.7 antibody before shear. The antibody produced a marked reduction in the extent of aggregation. It should be noted that the fraction of multiplets in the case of neutrophils preincubated without the antibody is significantly greater than that shown in Fig. 6 (*left*) for neutrophils sheared immediately after 1 min to allow warming up to room temperature.

s⁻¹ (32.8% s⁻¹) was comparable to that in suspensions sheared at higher shear stress in 10% Ficoll, the extent of aggregation was significantly lower, decreasing by 41 and 21% at $G = 110$ and 220 s⁻¹, respectively. Moreover, there was a considerable decrease in aggregate growth compared to that at the higher shear stress, the fraction of cells in doublets and triplets now exceeding those found in multiplets.

To eliminate the possibility that the above-described rapid and extensive aggregation might not occur in the absence of the viscous cosolvent, Ficoll-400, experiments were also carried out with the cells suspended in the Tyrodes buffer, $\eta = 1.01$ mPa s (22°C), with the shear stress now reduced to 0.11 Pa at $G = 110$ s⁻¹. Although the time to sediment from mid-plane to the lower plate was now reduced to 10 s, we observed qualitatively the same rapid aggregation and formation of multiplets of neutrophils that were seen within 5 s of shear in 5 and 10% Ficoll.

Effect of anti-CD18 (R15.7)

The effect of incubating the suspension of neutrophils for 5 min with 10 μ g/ml of the antibody R15.7 against β_2 -integrins before shearing was tested at $G = 110$ and 220 s⁻¹. Figure 7 shows the distribution of aggregates at 10.8 s, compared to that in controls with no added antibody. Clearly, blocking CD18 with antibody significantly sup-

pressed the extent and the growth of multicellular aggregates, the percent neutrophils in aggregates decreasing by 48 and 37% at $G = 110$ and 220 s^{-1} , respectively, and the proportion of cells in multiplets decreasing by 83 and 75%, respectively.

Effect of chemotactic stimulation

The above results demonstrate that, in addition to L-selectin, β_2 -integrins are required for multicellular aggregate formation. Therefore, we carried out some experiments with neutrophils stimulated with fMLP to examine the effect of a likely much larger number of activated β_2 -integrins on the kinetics of aggregation. Neutrophil suspensions were incubated with 200 pM fMLP for 3 min at room temperature before shearing at $G = 110$ and 220 s^{-1} . Table 2 shows that, unlike unstimulated neutrophils, the addition of fMLP results in significant numbers (6%) of nonseparating doublets and an increase in the mean doublet lifetime even at $G = 14 \text{ s}^{-1}$. As illustrated in Fig. 5 c, at $G = 110 \text{ s}^{-1}$, there was a large increase in the initial rate ($23.5\% \text{ s}^{-1}$) and extent of aggregation (27.7%) from that in unstimulated cells (Fig. 5 A). The increase was accompanied by an increase in the rate of large aggregate growth (not shown). More importantly, as shown below, the rates of disaggregation were significantly slower than those in suspensions of unstimulated neutrophils.

Rates of disaggregation

The break-up of aggregates in 10% Ficoll was studied by rapidly reducing the rate of shear after 10 s at $G = 110$ and 220 s^{-1} . The results are shown in Fig. 8 a by plots of the percent neutrophils in aggregates versus time of shear at low G .

The effect of chemotactic stimulation in preventing disaggregation upon reducing the shear rate is shown in Fig. 8 b, in which unstimulated cells are compared with cells stimulated with $1 \mu\text{M}$ fMLP. It should be noted that, in these suspensions activated with $1 \mu\text{M}$ fMLP, there was no significant shedding of L-selectin after 1 min of shear at $G = 110 \text{ s}^{-1}$ as seen by flow cytometry. The suspensions were initially sheared at $G = 110 \text{ s}^{-1}$ before rapidly reducing G to 14 s^{-1} and then again rapidly raising G to 110 s^{-1} . Whereas the unstimulated cells showed rapid disaggregation, which was again rapidly reversed on reapplying a high shear rate, the fMLP-activated cells showed almost no disaggregation.

DISCUSSION

Two-stage aggregation

A remarkable result of this study of shear-induced collisions between unstimulated neutrophils was the large extent of

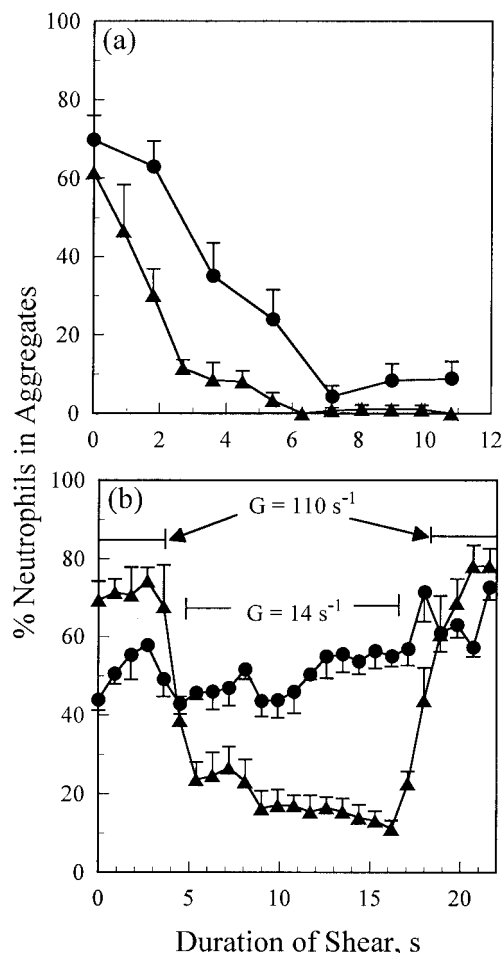


FIGURE 8 Rates of disaggregation. (a) Suspensions of unstimulated neutrophils in 10% Ficoll were sheared for 10 s at $G = 110$ (●) and 220 s^{-1} (▲), respectively, and the shear rate rapidly reduced to $G = 14 \text{ s}^{-1}$ within 3 s. Plot of the percent neutrophils in aggregates against time beginning at the moment when the shear rate was reduced. The slower initial rate of disaggregation at $G = 220 \text{ s}^{-1}$ ($3.7\% \text{ s}^{-1}$) than at $G = 110 \text{ s}^{-1}$ ($16.5\% \text{ s}^{-1}$) is likely due to the additional time, $\sim 2 \text{ s}$, required to reduce the shear rate to below 66 s^{-1} . Thereafter, the rates are comparable. (b) Suspensions of unstimulated neutrophils (▲), and those stimulated immediately before shearing with $1 \mu\text{M}$ fMLP (■) were first sheared at $G = 110 \text{ s}^{-1}$ for 3 s before reducing G to 14 s^{-1} and maintaining it for 10 s. The shear rate was then rapidly restored to 110 s^{-1} . Whereas the unstimulated cells exhibited a rapid disaggregation that was reversed upon reapplication of high shear rate, the stimulated cells exhibited almost no disaggregation.

aggregation occurring as the shear rate exceeded a threshold value of 66 s^{-1} . Thus, already in the first second or two of shear, a significant fraction of the two-body collisions observed in the rheoscope resulted in the formation of nonseparating doublets that remained intact as they rotated through the quadrant $0 < \phi_1 < 90^\circ$ in which they were subjected to tensile force. As a result, the measured two-body-collision capture efficiencies were greater than 20% at $G = 110$ and 220 s^{-1} . The values of ε and the fact that most of the doublets rapidly grew into multiplets in less than 5 s,

are in agreement with the results reported by Taylor et al. (1996) and Neelamegham et al. (1997). In those studies, the capture efficiency increased linearly with shear stress up to 40% at $G = 400 \text{ s}^{-1}$. (Values of the collision efficiency given by Taylor et al. (1996) were subsequently corrected, divided by a factor of 2, as described in Neelamegham et al. (2000).) A key difference is that, in the previous studies, aggregation was measured in the presence of a potent dose of chemotactic stimulus ($1 \mu\text{M}$ fMLP) and the kinetics of doublet, triplet, and multiplet formation were obtained by fixing samples in glutaraldehyde, subsequently analyzing the particle size distribution by fluorescence flow cytometry. That work led to the emergence of a coherent two-stage model of the molecular dynamics underlying aggregation. In the first stage, the L-selectin–PSGL-1 bonds function to increase the contact time between colliding cells, and this was found to be strongly shear rate-dependent, as we have observed in the absence of activators. In fact, in the present work, L-selectin adhesive bonds at $G \geq 110 \text{ s}^{-1}$ were sufficient to keep as many as 25% of collision doublets intact over 0.6 to >6 rotational orbits, corresponding to adhesive lifetimes ranging from 0.1 to 1 s. In the second stage, the increased contact time of colliding cells facilitates the binding of β_2 -integrins, and thus supports the formation of stable aggregates. In the case of chemotactically stimulated neutrophils, such aggregates can remain intact over minutes.

The molecular cooperativity associated with the transition from selectin- to integrin-dependent aggregation was also confirmed in the present study, because the aggregation was effectively suppressed by anti-L-selectin antibodies, and was significantly reduced (very few multicellular aggregates) by the anti-CD18 antibody. There is good evidence that ligation and cross-linking of L-selectin results in signaling of neutrophil adhesion function (Simon et al., 1995; Downey et al., 1996; Tsang et al., 1997). One of us has recently reported on a novel mechanism by which neutrophil rolling via L-selectin and PSGL-1 led to activation of β_2 -integrins and firm adhesion to an ICAM-1 expressing cell substrate (Simon et al., 2000). The transition from selectin-mediated tethering to integrin-dependent stable adhesion required the application of a steady shear flow in a parallel-plate flow chamber. There was also evidence for intracellular signaling of adhesion, since a specific inhibitor of phosphorylation of p38 MAP kinase blocked upregulation and adhesion via β_2 -integrins. Several critical aspects of these studies on L-selectin-dependent signaling are reflected in the current observations of neutrophil homotypic aggregation.

Nevertheless, one can ask the question that, if there is indeed signaling leading to activation of β_2 -integrins and the formation of more stable bonds, why do all the aggregates break up on reducing the shear rate? It has been shown that stimulation of neutrophils by cross-linking of L-selectin with monoclonal antibody results in a transient activation of

β_2 -integrin adhesion (Gopalan et al., 1997). It is therefore not unreasonable to postulate that shear stress-induced tethering via L-selectin between neutrophils can result in transient signaling and activation of β_2 -integrin. The efficiency of such signaling would be expected to be dependent on the number of L-selectin bonds, a function of the area of adhesive contact and on the number of β_2 -integrin molecules in proximity to the ligand, both dependent on the maintenance of shear.

Aggregation requires maintenance of shear

Although the formation of aggregates as observed in the rheoscope did not require chemotactic stimulation, maintenance of a threshold level shear rate was necessary. Thus, we found that, at the lower shear rate of 66 s^{-1} , almost only doublets and a few triplets formed, whereas at shear rates of 110 s^{-1} and 220 s^{-1} aggregates ranging from doublets to multiplets of 15 or more cells were formed, the latter comprising as many as 62 and 94% of cells in aggregates, respectively. However, as the shear rate was lowered below 66 s^{-1} , within a second or two, the multiplets disaggregated, followed by most of the doublets and triplets as the shear rate reached 14 s^{-1} . Even when shear was maintained over one minute, the percent neutrophils in multiplets decreased after 10 s, although the percent neutrophils in aggregates remained constant by a subsequent increase in the number of doublets and triplets. By contrast, in the presence of $1 \mu\text{M}$ fMLP, the percent aggregation at $G = 100$ and 400 s^{-1} measured by Taylor et al. (1996) increased to a maximum after 200 and 100 s of shear, respectively.

These observations may account for the low degree of aggregation observed for unstimulated neutrophils, $\leq 5\%$ formation of small aggregates, measured by Taylor et al. (1996) at $G > 100 \text{ s}^{-1}$ as compared to $>50\%$ including a high fraction of multiplets, reported in the present work. The difference is not accounted for by the higher concentration of neutrophils used in the present work, $\geq 15,000 \mu\text{l}^{-1}$ compared to $1000 \mu\text{l}^{-1}$ in the previous work. In that study, the collision efficiency for unstimulated neutrophils computed over the initial 5 s of shear using Eq. 6 was 0.5%, compared to $\varepsilon > 20\%$ over 5 s found in the present work. The difference likely lies in the sampling protocol applied in previous studies using the cone-plate viscometer, which involved briefly arresting the shear while sample was removed. The cessation of shear flow presumably led to the break-up of aggregates upon sampling. Such break-up would not be expected to occur with fMLP-stimulated neutrophils, because, with chemotactic activation of many β_2 -integrin bonds having longer lifetimes, stable aggregates would form, and these were seen and measured in the cone-plate studies. Indeed, experiments carried out in the present investigation with neutrophils in the presence of $1 \mu\text{M}$ fMLP showed an almost complete absence of disaggregation upon reducing the shear rate. Even in the case of

neutrophils pre-incubated with only 200 pM fMLP, up to 27% of cells remained in aggregates after reducing the shear rate.

Mechanism of shear dependence of aggregation

One mechanism proposed for a shear rate-dependent selectin bond formation stems from the observation by Finger et al. (1996) of a threshold shear rate effect similar to the one described here. This occurred in a study of L-selectin adhesion, including L-selectin-dependent neutrophil rolling on neutrophils bound to an E-selectin substrate. It was found that, when reducing the wall shear stress from 0.15 to 0.03 Pa, the rolling neutrophils detached from the substrate and flowed freely. These authors postulate that, upon formation of the first short-lived bond between cell and substrate, the shear flow provides the transport that promotes additional L-selectin bonds to form. This may occur by bringing further microvilli, on which L-selectin molecules are clustered, in contact with the substrate. The increase in bond dissociation rate with increasing shear stress (Alon et al., 1995) is then compensated by a shear rate-dependent increase in the number of bonds per rolling step (Chen and Springer, 1999), thereby enabling rolling to continue over a wide range of wall shear stress. The authors argue that it is precisely the short lifetime of the L-selectin bond, compared to those of P-selectin and E-selectin (Alon et al., 1998), that is responsible for the uniqueness of the level of the shear stress requirement for L-selectin adhesion bonds.

There is another physical mechanism that can account for the existence of a threshold shear rate for the formation of L-selectin-PSGL-1 bonds as seen in this study, which is also applicable to the rolling of neutrophils in the experiments of Finger et al. (1996). It is based on theoretical considerations of Brownian dynamics (Kramers, 1940) and shows that, for bonds with complex potentials of mean force, the reverse reaction rate of a single bond is governed by the applied force on the bond, because this will determine what transition state dominates the unbinding (Evans and Ritchie, 1997; Merkel et al., 1999). Additional support for a physical mechanism underlying a threshold shear rate effect comes from experiments on the rolling of latex spheres bearing sialyl Lewis^x ligand (sLe^x) on L-selectin-covered surfaces in a parallel-plate flow chamber (Greenberg et al., 2000). Here, a threshold effect was seen in the absence of cellular features such as deformability or topography as its cause.

Evans and coworkers have shown that, for weak noncovalent receptor–ligand bonds, a dynamic spectrum of bond strengths is predicted as the rate at which a tensile force is applied is altered. The measured bond strength, defined as the force that produces the most frequent failure in repeated breakage tests, is governed by the prominent barriers traversed in the energy landscape along the force-driven dissociation pathway (Evans and Ritchie, 1997; Evans, 1998). Merkel et al. (1999), using a sophisticated biomembrane

force probe, studied bond formation between (strept)avidin and biotin, and were able to show that, as the loading rate increased over 6 orders of magnitude, the time for bond detachment decreased from about 1 min to 1 ms. At the same time, the rupture force increased from about 5 to 170 pN. The effect of loading rate on the force required for bond rupture has since been demonstrated in the case of single bonds formed between PSGL-1 linked to glass beads and L-selectin on neutrophils using the biomembrane force probe (Evans, 1998; Evans et al., 2001). The rates of dissociation of single bonds to L-selectin increased nearly 1000 fold as the rupture force rose from a few piconewtons to ~200 pN. The results revealed two prominent energy barriers along the bond-dissociation pathway, one above strengths of 75 pN arising from rapid detachment, <10 ms, impeded by an inner barrier, and the other at strengths less than 75 pN arising from slow dissociation, >10 ms, impeded by an outer barrier. The strong inner barrier was found to involve Ca⁺⁺ bonds between a single sLe^x and the lectin domain of the L-selectin. The weak outer barrier correlated with weak hydrogen bonds to sLe^x on PSGL-1 (Evans et al., 2001).

In the experiments described in this paper, the normal force loading rate, dF_n/dt given by differentiation of Eq. 5,

$$\frac{dF_n}{dt} = 2\alpha_n \eta G b^2 \left[\sin \theta_1 \cos \theta_1 \sin 2\phi_1 \frac{d\theta_1}{dt} + \sin^2 \theta_1 \cos 2\phi_1 \frac{d\phi_1}{dt} \right], \quad (9)$$

is maximal at $\phi_1 = 0^\circ$, when the tensile force (Eq. 5) is zero, and zero at $\phi_1 = 45^\circ$ when F_n is maximal. The times spent by the doublet under tensile-force loading, from $0 \leq \phi_1 \leq 45^\circ$, as calculated from the integrated form of Eq. 3, is 10.6 and 5.3 ms at $G = 110$ and 220 s^{-1} . The results of the biomembrane force probe experiments (Evans et al., 2001) clearly indicate that the above tensile force intervals are significantly longer than the times for single L-selectin-PSGL-1 bonds to dissociate (~1.5 and 0.2 ms, respectively) at the corresponding mean values of F_n (139 and 278 pN, respectively) during the period of tensile-force loading (maximum loading rates = 3.33×10^4 and $6.66 \times 10^4 \text{ pN s}^{-1}$, respectively). (F_n and dF_n/dt were computed using $\alpha_n = 19.2$ for h estimated to be ~50 nm (Arp and Mason, 1977) and $b = 4.35 \text{ }\mu\text{m}$. The values of the angle factor $\sin^2 \theta_1 \sin 2\phi_1$ in Eq. 5 were computed from the integrated forms of Eqs. 2 and 3 with the mean value of the orbit constant (integration constant; Tees et al., 1993) $C = 4.27$ previously given by Kwong et al. (1996) for a population of rotating doublets of latex spheres.) However, if multiple bonds were formed during a collision, the time to dissociate would increase as they were broken successively by a zipper-like dissociation of successive selectin bonds (Evans et al., 2001). The opportunity for multiple bond formation

would occur as the cells come into close proximity under a sufficiently high compressive normal force in the quadrant $-90^\circ \leq \phi_1 \leq 0^\circ$, when the cells may be flattened and an area of contact of the order of $5\text{--}10 \mu\text{m}^2$ could develop in a matter of a millisecond (Evans et al., 2001). Assuming a uniform distribution of receptor sites in neutrophils having surface area $\sim 240 \mu\text{m}^2$, a contact area of $5 \mu\text{m}^2$ would have ~ 200 PSGL-1 and ~ 1000 L-selectin molecules (Moore et al., 1991; Taylor et al., 1996). As the bonds are subjected to tensile normal force in the quadrant $0^\circ \leq \phi_1 \leq 45^\circ$, the time, t_c , for the contact area to relax can be estimated from the turgor pressure, P_c , of the neutrophil (of the order of 10 N/m^2 ; Evans and Yeung, 1989) and its internal viscosity η_{pmm} (of the order of 10 Pa s): $t_c = \eta_{\text{pmm}}/P_c = 1 \text{ s}$. This interval for relaxation is much greater than the mean time under tensile force in our experiments ($< 10.6 \text{ ms}$) and thus the contact area has insufficient time to relax during the unloading phase, and is essentially unchanging during the rotational orbit.

That we observe a threshold shear rate for significant collision efficiencies to occur (corresponding to a maximum bond-loading rate $\sim 2 \times 10^4 \text{ pN s}^{-1}$) could be explained by the existence of a threshold rate of compression-force loading. Below this threshold, the rate of formation of the contact area is not rapid enough to allow sufficient numbers of bonds to form. This notion is supported by the fact that the mean doublet lifetimes, capture efficiencies, and extents of aggregation in 5% Ficoll are significantly lower than in 10% Ficoll, where there is a 50% reduction in the compression-force loading rates due to lower shear stress.

Shear-induced cell deformation

At the magnifications used in the present study, it was impossible to detect flattening of a membrane area of $5\text{--}10 \mu\text{m}^2$, and no gross deformation of single neutrophils was seen, even at $G = 220 \text{ s}^{-1}$ in 10% Ficoll (shear stress = 1.21 Pa). However, such deformation, even if small, would be detectable through the measured period of rotation, T . We have previously shown that, in the case of doublets of sphered and aldehyde-fixed red cells cross-linked by antibody, the measured dimensionless period of rotation, TG , was close to the value of 15.62 (Tha and Goldsmith, 1986; Tees et al., 1993), predicted for rigidly linked touching spheres (Takamura et al., 1979; Wakiya, 1971). Thus, the spheres, although estimated to be separated by a distance $h = 20 \text{ nm}$, did not rotate independently of each other. By contrast, measurements of TG for nonseparating neutrophil doublets chosen in randomly selected sequences at $G = 110$ and 220 s^{-1} , gave a mean value of $TG = 16.53 \pm 0.85$ (SD, $n = 50$), with some values as high as 18. The increase in TG from 15.62 could be due to the increased distance between neutrophil membranes because of the microvilli, estimated to have average lengths of $0.3 \mu\text{m}$ (Shao et al., 1998). If the doublet were bonded between two microvilli tips, i.e., $h =$

$0.6 \mu\text{m}$, theory predicts that TG would increase to 15.98 for rigidly linked spheres. If then, the spheres were free to independently rotate, TG would increase further, with the magnitude of the increase depending on the degree of freedom to rotate (Table 1 in Adler et al., 1981). However, given the likelihood of microvilli compression leading to multiple bond formation between cells, bonding between uncompressed microvilli would be infrequent. It may be more likely in collisions at low ϕ_1^0 . A more plausible explanation for the higher mean TG is to postulate a small shear stress-induced deformation of the neutrophils into prolate spheroids. The above value of $TG = 16.53$ corresponds to the rotation of a doublet with an equivalent ellipsoidal axis ratio, $r_e = 2.17$. In such a doublet each cell would be slightly deformed into an ellipsoid of axis ratio 1.04, a deformation difficult to detect. To solve this problem and, more importantly, to determine the extent of cell flattening during two-body collisions and its dependence on shear rate, it will be necessary to examine electron micrographs of singlets and doublets obtained from suspensions to which aldehyde has been added during shear. We intend to pursue this line of investigation.

Tether formation

It has been hypothesized in neutrophil rolling (Shao et al., 1998) that, at a mechanical load of $> 64 \text{ pN}$ on a selectin bond, its microvillus anchorage point will stretch and that this will actually shield the bond from the full effect of the increased shear force. In the present experiments, the maximum tensile and compressive normal forces acting on doublets of neutrophils at $G = 110$ and 220 s^{-1} was much higher than 64 pN . Following compression, there might be stretching of the microvilli during rotation from $\phi_1 = 0^\circ$ to $\phi_1 = +90^\circ$ which could result in membrane tether formation. Formation of thin membrane tethers during neutrophil attachment to spread platelets on the surface of a parallel-plate chamber has recently been described in detail (Schmidtke and Diamond, 2000). Yet, such stretching of the microvillus anchorage point appears less likely with freely suspended neutrophils. Here, the molecular point attachments are not anchored to a stationary surface, because the cells rotate together, and tensile and compressive normal forces vary rapidly and periodically in each half orbit.

Nevertheless, we occasionally observed the rotation of doublets of cells whose surfaces were separated by clear suspending fluid, and in which the inter-surface distance varied with doublet orientation. Apparently, the cells were linked by a flexible fiber not visible under the microscope. Here, the values were $TG > 18.5$, indicating that the individual neutrophils were capable of independent rotation (van de Ven and Mason, 1976; Takamura et al., 1979; 1981b). Such doublets, although few in number, would likely have been formed through linkages between interact-

ing microvilli, and the tethers developed in the tensile phases of successive rotational orbits.

Distribution of lifetimes of transient doublets

Contrary to expectations, the mean distribution in the lifetimes of transient doublets in control suspensions containing 2 mM EDTA were not smaller than those predicted for collision doublets of noninteracting smooth spheres. Table 2 shows that fully 50.9 and 38.5% of the transient doublets continued to rotate past the mirror image of the apparent angle of approach, $\Delta\phi_2 > 0^\circ$, at $G = 110$ and 220 s^{-1} , respectively. It could be that there are nonspecific interactions between the neutrophils that account for this result. These would be expected to decrease in strength with increasing shear rate; indeed a small fraction of nonseparating doublets were found at $G = 110 \text{ s}^{-1}$ and these disappeared at higher G . At the same time, the fraction of doublets having $\Delta\phi_2 < 0^\circ$ increased with increasing shear rate. An alternate explanation might involve geometric considerations of microvilli interactions, such as their interdigitation during rotation, allowing for greater membrane-to-membrane contact.

Concluding remarks

Several lines of evidence indicate that the L-selectin bond works more efficiently in transiently tethered cells over a particular range of fluid shear rate. In the context of neutrophil homotypic interactions, we observed an enhanced formation of aggregates above a threshold level of shear rate. It is possible that this amplification in adhesion efficiency is related to an increase in the rate of loading of the L-selectin bond, resulting in an order-of-magnitude greater force required to rupture a single bond and to the formation of multiple bonds. A significant finding in these studies is evidence that there is recruitment of β_2 -integrin bonds and formation of stable aggregates at shear rates above the threshold level. These data provide further evidence for the dynamic signaling of adhesion function upon engagement of L-selectin over time intervals from 18 to 60 ms, time intervals that would be relevant to homotypic aggregation and heterotypic capture on the endothelium of the microcirculation.

This work was supported by grant MT-13617 from the Medical Research Council of Canada, a grant from the Quebec Heart and Stroke Foundation. S.I.S. was supported by National Institutes of Health grant AI 47294 and is an established investigator of the American Heart Foundation.

The authors are much indebted to Dr. Evan Evans for discussion and advice concerning the mechanism of homotypic neutrophil aggregation. We thank Eberhard Beier of Carl Zeiss Canada Ltd. for his excellent work on the construction of a microscope stage to house the rheoscope.

REFERENCES

- Abassi, O., T. K. Kishimoto, L. V. McIntire, D. C. Anderson, and C. W. Smith. 1993. E-Selectin supports neutrophil rolling under conditions of flow. *J. Clin. Invest.* 93:2719–2730.
- Adler, P. M., K. Takamura, H. L. Goldsmith and S. G. Mason. 1981. Particle motions in sheared suspensions. XXX. Rotations of rigid and flexible dumbbells (theoretical). *J. Colloid Interface Sci.* 83:502–515.
- Alon, R., D. A. Hammer, and T. A. Springer. 1995. Lifetime of the P-selectin–carbohydrate bond and its response to tensile force in hydrodynamic flow. *Nature.* 374:539–542.
- Alon, R., S. Chen, K. D. Puri, E. B. Finger, and T. A. Springer. 1998. The kinetics of L-selectin tethers and the mechanics of selectin-mediated rolling. *J. Cell Biol.* 138:1169–1180.
- Arp, P., and S. G. Mason. 1976. Orthokinetic collisions of hard spheres in simple shear flow. *Can. J. Chem.* 54:3760–3774.
- Arp, P. A., and S. G. Mason. 1977. The kinetics of flowing dispersions. VIII. Doublets of rigid spheres (theoretical). *J. Colloid Interface Sci.* 61:21–43.
- Atherton, A., and G. V. R. Born. 1973. Relationship between the velocity of rolling granulocytes and that of blood flow in venules. *J. Physiol.* 233:157–165.
- Bargatze, R. F., S. Kurk, E. C. Butcher, and M. A. Julita. 1994. Neutrophils roll on adherent neutrophils bound to cytokine-induced endothelial cells via L-selectin on the rolling cells. *J. Exp. Med.* 189:1785–1792.
- Bartok, W., and S. G. Mason. 1957. Particle motions in sheared suspensions. V. Rigid rods and collision doublets of spheres. *J. Colloid Sci.* 12:243–262.
- Batchelor, G. K., and J. T. Green. 1972. The hydrodynamic interaction of two small freely moving spheres in a linear flow field. *J. Fluid Mech.* 56:375–400.
- Chen, S., and T. A. Springer. 1999. An automatic braking system that stabilizes leukocyte rolling by an increase in selectin bond number with shear. *J. Cell Biol.* 144:185–200.
- Curtis, A. S. G., and L. M. Hocking. 1970. Collision efficiency of equal spherical particles in a shear flow. The influence of London–van der Waals forces. *Trans. Faraday Soc.* 66:1381–1390.
- Downey, G. P., J. R. Butler, J. Brumell, N. Borregaard, L. Kjeldson, A. K. Sue-A-Quan, and S. Grinstein. 1996. Chemotactic peptide-induced activation of MEK-2, the predominant isoform in human neutrophils. Inhibition by wortmannin. *J. Biol. Chem.* 271:21005–21011.
- Evans, E. 1998. Energy landscapes of biomolecular adhesion and receptor anchoring at interfaces explored with dynamic force spectroscopy. *Faraday Discuss.* 111:1–16.
- Evans, E., and K. Ritchie. 1997. Dynamic strength of molecular adhesion bonds. *Biophys. J.* 72:1541–1555.
- Evans, E., and A. Yeung. 1989. Apparent viscosity and cortical tension of blood granulocytes determined by micropipet aspiration. *Biophys. J.* 56:151–160.
- Evans, E., A. Leung, D. Hammer, and S. I. Simon. 2001. Chemically distinct transition states govern rapid dissociation of single L-selectin bonds under force. *Proc. Natl. Acad. Sci. U.S.A.* 98:3784–3789.
- Finger, E. B., D. P. Kamal, R. Alon, M. B. Lawrence, U. H. von Andrian, and T. A. Springer. 1996. Adhesion through L-selectin requires a threshold hydrodynamic shear. *Nature.* 379:266–269.
- Goldsmith, H. L., and S. G. Mason. 1967. The microrheology of dispersions. In *Rheology: Theory and Applications*. Vol. 4. F. R. Eirich, editor. Academic Press, Inc., New York. 85–250.
- Goldsmith, H. L., O. Lichtarge, M. Tessier Lavigne, and S. Spain. 1981. Some model experiments in hemodynamics. VI. Two-body collisions between blood cells. *Biorheology.* 18:532–555.
- Gopalan, P. K., C. W. Smith, H. Lu, E. L. Berg, L. V. McIntire, and S. I. Simon. 1997. Neutrophil CD18-dependent arrest on ICAM-1 in shear flow can be activated through L-selectin. *J. Immunol.* 158:367–375.
- Greenberg, A. W., D. K. Brunk, and D. A. Hammer. 2000. Cell-free rolling mediated by L-selectin and sialyl Lewis^x reveals the shear threshold effect. *Biophys. J.* 79:2391–2402.

- Guyer, D. A., K. L. Moore, E. B. Lynam, C. M. Schammel, S. Rogelj, R. P. McEver, and L. A. Sklar. 1996. P-selectin glycoprotein ligand (PSGL-1) is a ligand for L-selectin in neutrophil aggregation. *Blood*. 88: 2415–2421.
- Hentzen, E. R., S. Neelamegham, G. S. Kansa, J. A. Benanti, L. V. McIntire, C. W. Smith, and S. I. Simon. 2000. Sequential binding of CD11a/CD18 and CD11b/CD18 defines neutrophil capture and stable adhesion to intercellular adhesion molecule-1. *Blood*. 95:911–920.
- Jeffery, G. B. 1922. On the motion of ellipsoidal particles immersed in a viscous fluid. *Proc. R. Soc. (Lond.) A*. 102:162–179.
- Jones, D. A., O. Abassi, L. V. McIntire, R. P. McEver, and C. W. Smith. 1993. P-selectin mediates neutrophil rolling on histamine-stimulated endothelial cells. *Biophys. J.* 65:1560–1569.
- Kramers, H. A. 1940. Brownian motion in a field of force and the diffusion model of chemical reactions. *Physica (Utrecht)*. 7:284–304.
- Kwong, D., D. F. J. Tees, and H. L. Goldsmith. 1996. Kinetics and locus of failure of receptor–ligand mediated adhesion between latex spheres. II. Protein–protein bond. *Biophys. J.* 71:1115–1122.
- Long, M., H. L. Goldsmith, D. F. J. Tees, and C. Zhu. 1999. Probabilistic modeling of shear-induced formation and breakage of doublets cross-linked by receptor–ligand bonds. *Biophys. J.* 1112–1128.
- Merkel, R., P. Nassoy, A. Leung, K. Ritchie, and E. Evans. 1999. Energy landscapes of receptor–ligand bonds explored with dynamic force spectroscopy. *Nature*. 397:50–53.
- Moore, K. L., A. Varki, and R. P. McEver. 1991. GMP-140 binds to a glycoprotein receptor on human neutrophils: evidence for a lectin-like interaction. *J. Cell Biol.* 112:491–499.
- Neelamegham, S., A. D. Taylor, J. D. Hellums, M. Dembo, C. W. Smith, and S. I. Simon. 1997. Modeling the reversible kinetics of neutrophil aggregation under hydrodynamic shear. *Biophys. J.* 72:1527–1540.
- Neelamegham, S., A. D. Taylor, H. Shankaran, C. W. Smith, and S. I. Simon. 2000. Shear and time-dependent changes in Mac-1, LFA-1, and ICAM-3 binding regulate neutrophil homotypic adhesion. *J. Immunol.* 164:3798–3805.
- Okuyama, M., J. Kambayashi, M. Sakon, and M. Monden. 1996. LFA-1/ICAM-3 mediates neutrophil homotypic aggregation under fluid shear stress. *J. Cell. Biochem.* 60:550–559.
- Rochon, Y. P., and M. M. Frojmovic. 1991. Dynamics of human neutrophil aggregation evaluated by flow cytometry. *J. Leukoc. Biol.* 50:434–443.
- Shao, J.-Y., H. P. Ting-Beall, and R. M. Hochmuth. 1998. Static and dynamic lengths of neutrophil microvilli. *Proc. Natl. Acad. Sci. U.S.A.* 95:6797–6802.
- Schmidtke, D. W., and S. L. Diamond. 2000. Direct observation of membrane tethers formed during neutrophil attachment to platelets or P-selectin under physiological flow. *J. Cell Biol.* 149:719–730.
- Simon, S. I., J. D. Chambers, and L. A. Sklar. 1990. Flow cytometric analysis and modeling of cell–cell adhesive interactions: the neutrophil as a model. *J. Cell Biol.* 111:2747–2756.
- Simon, S. I., A. R. Buns, A. D. Taylor, P. K. Gopalan, E. B. Lyman, and L. A. Sklar. 1995. L-selectin (CD62L) cross-linking signals neutrophil adhesive functions via the Mac-1 (CD11b/CD18) β_2 integrin. *J. Immunol.* 155:1502–1514.
- Simon, S. I., D. Vestweber, and C. W. Smith. 2000. Neutrophil tethering on E-selectin activates beta 2 integrin binding to ICAM-1 through a mitogen activated protein kinase signal transduction pathway. *J. Immunol.* 164:4348–4358.
- Springer, T. A. 1994. Traffic signals for lymphocyte recirculation and leukocyte emigration: the multistep paradigm. *Cell*. 76:301–314.
- Swift, D. L., and S. K. Friedlander. 1964. The coagulation of hydrosols by Brownian motion and laminar shear flow. *J. Colloid Sci.* 19:621–647.
- Takamura, K., H. L. Goldsmith, and S. G. Mason. 1979. The microrheology of colloidal dispersions. IX. Effects of simple and polyelectrolytes on rotation of doublets of spheres. *J. Colloid Interface Sci.* 72:385–400.
- Takamura, K., H. L. Goldsmith, and S. G. Mason. 1981a. The microrheology of colloidal dispersions. XII. Trajectories of orthokinetic pair-collisions of latex spheres in a simple electrolyte. *J. Colloid Interface Sci.* 82:175–189.
- Takamura, K., P. M. Adler, H. L. Goldsmith, and S. G. Mason. 1981b. Particle motions in sheared suspensions. XXX. Rotations of rigid and flexible dumbbells (experimental). *J. Colloid Interface Sci.* 83:516–530.
- Tandon, P., and S. L. Diamond. 1997. Hydrodynamic effects and receptor interactions of platelets and their aggregates in linear shear flow. *Biophys. J.* 73:2819–2835.
- Tandon, P., and S. L. Diamond. 1998. Kinetics of β_2 -integrin and L-selectin bonding during neutrophil aggregation in shear flow. *Biophys. J.* 75:3163–3178.
- Taylor, A. D., S. Neelamegham, J. D. Hellums, C. W. Smith, and S. I. Simon. 1996. Molecular dynamics of the transition from L-selectin- to β_2 -integrin-dependent neutrophil adhesion under defined hydrodynamic shear. *Biophys. J.* 71:3499–3500.
- Tees, D. F. J., O. Coenen, and H. L. Goldsmith. 1993. Interaction forces between red cells agglutinated by antibody. IV. Time and force dependence of break-up. *Biophys. J.* 65:1318–1334.
- Tees, D. F. J., and H. L. Goldsmith. 1996. Kinetics and locus of failure of receptor–ligand mediated adhesion between latex spheres. I. Protein–carbohydrate bond. *Biophys. J.* 71:1102–1114.
- Tha, S. P., and H. L. Goldsmith. 1986. Interaction forces between red cells agglutinated by antibody. I. Theoretical. *Biophys. J.* 50:1109–1116.
- Tsang, Y. T., S. Neelamegham, Y. Hu, E. L. Berg, A. R. Burns, C. W. Smith, and S. I. Simon. 1997. Synergy between L-selectin signaling and chemotactic activation during neutrophil adhesion and transmigration. *J. Immunol.* 1159:4566–4577.
- van de Ven, T. G. M. 1989. *Colloidal Hydrodynamics*. Academic Press, San Diego.
- van de Ven, T. G. M., and S. G. Mason. 1976. The microrheology of colloidal dispersions. IV. Pairs of interacting spheres in shear flow. *J. Colloid Interface Sci.* 57:505–516.
- van de Ven, T. G. M., and S. G. Mason. 1977. The microrheology of colloidal dispersions. VII. Orthokinetic doublet formation of spheres. *Colloid Polymer Sci.* 255:468–479.
- Vestweber, D., and J. E. Blanks. 1999. Mechanisms that regulate the function of the selectins and their ligands. *Physiol. Rev.* 79:181–213.
- von Andrian, U. H., P. Hansell, J. D. Chambers, E. M. Berger, I. Torres Filno, E. C. Butcher, and K. E. Arfors. 1992. L-selectin function is required for beta 2-integrin-mediated neutrophil adhesion at physiological shear rates in vivo. *Am. J. Physiol. Heart Circ. Physiol.* 263: H1034–H1044.
- von Adrian, U. H., J. D. Chambers, E. L. Berg, S. A. Michie, D. A. Brown, D. Karolak, L. Ramezani, E. M. Berger, K. E. Arfors, and E. C. Butcher. 1993. L-selectin mediates neutrophil rolling in inflamed venules through sialyl Lewis^x-dependent and -independent recognition pathways. *Blood*. 82:182–191.
- von Smoluchowski, M. 1917. Versuch einer mathematischen Theorie der Koagulationskinetik kolloider Lösungen. *Z. Phys. Chem.* 92:129–168.
- Wakiya, S. 1971. Slow motion in shear flow of a doublet of two spheres in contact. *J. Phys. Jpn.* 31:1581–1587. (errata, 1972, 33:278).
- Walchek, B., K. L. Moore, R. P. McEver, and T. K. Kishimoto. 1996. Neutrophil–neutrophil interactions under hydrodynamic shear stress involve L-selectin and PSGL-1: a mechanism that amplifies initial leukocyte accumulation of P-selectin in vitro. *J. Clin. Invest.* 98:1081–1087.